

Balance between resource supply and demand determines nutrient limitation of primary productivity in the ocean

George I. Hagstrom¹, Simon A. Levin¹ & Adam C. Martiny^{2,3}

¹*Department of Ecology and Evolutionary Biology, Princeton University*

²*Department of Earth Systems Science, University of California at Irvine*

³*Corresponding Author*

What is the ultimate limiting nutrient in the ocean? The dominant theory, which was first proposed by Redfield and later formalized by Tyrrell^{1,2}, states that despite the scarcity of fixed nitrogen in the surface ocean, phosphorus availability ultimately determines primary productivity. Two recent findings directly challenge the assumptions of the Redfield-Tyrrell paradigm: the discovery of systematic variations of phytoplankton N:P:Fe and widespread iron-limitation of phytoplankton. Here we use a simple model of nitrogen, phosphorus, and iron cycling to show how the resource demand ratios and biogeography of phytoplankton interact with resource supply ratios to govern nutrient cycling and primary productivity. We find that all three nutrients can limit global primary productivity, and that the ratio of geochemical supply to biological demand of each nutrient in each ocean region determines the limiting nutrients, with nitrogen fixation providing a mechanism for the cycles to interact. These results have important consequences for our understanding of biogeochemical cycles, ocean atmosphere interactions, marine ecology, and the response of ocean ecosystems to cli-

mate change. Our work demonstrates the importance of resource ratios and suggest that future studies of the physiological and geochemical regulation of these ratios are indispensable to building accurate theories and future predictions of nutrient cycling and primary productivity.

The modern view of marine biogeochemistry is that nitrogen is the *proximate* and phosphorus is the *ultimate limiting nutrient* in the ocean. Initially, biologists used the results of bottle enrichment experiments as evidence that fixed nitrogen limits primary productivity, as populations showed dramatic responses to nitrogen but rarely to other nutrients^{3,4}. A much different line of reasoning came from geochemists, who pointed out that the marine fixed nitrogen inventory is regulated by nitrogen fixation and denitrification, and that the availability of phosphorus may control the balance of these processes over geologic time-scales. These two ideas were reconciled by Tyrrell^{2,5,6}, who provided a simple mathematical model explaining how phosphorus-limited diazotrophs can homeostatically regulate nitrate and primary productivity. This model explained the Redfield-Tyrrell paradigm¹ by suggesting that the deficit between $(N:P)_{\text{deep}}$ and $(N:P)_{\text{org}}$ is due to a diazotroph growth penalty, leaving other phytoplankton perpetually nitrogen limited. According to this viewpoint, nitrogen is the *proximate limiting nutrient* and phosphorus is the *ultimate limiting nutrient*.

Two new discoveries challenge the Redfield-Tyrrell paradigm: the discovery of widespread iron-limitation^{7,8} and large scale systematic deviations of phytoplankton elemental stoichiometry⁹⁻¹¹. There is extensive evidence (as acknowledged by Tyrrell) that phytoplankton, particularly

nitrogen fixers, can be limited by iron in large parts of the oceans. Furthermore, surface phosphorus levels in subtropical gyres are anti-correlated with estimates of aeolian dust flux and local dissolved iron levels^{8,12,13}, which suggests that diazotrophs are only phosphorus-limited in high-iron regions such as the subtropical North Atlantic Ocean⁷. Iron limitation of diazotrophs points at iron, and not phosphorus, as the *ultimate limiting nutrient*. The discovery of latitudinal gradients in phytoplankton stoichiometry is challenging for homeostatic models of deep ocean nutrient levels. Recent surveys of $(N:P)_{org}$ ¹⁰ and nutrient tracers¹¹ show that $(N:P)_{org}$ has systematic variations throughout the ocean: with $(N:P)_{org} > 20$ in subtropical gyres and $(N:P)_{org} < 12$ in high-latitude regions. These patterns are not yet fully understood, but appear to be set by some combination of nutrient levels^{14,15}, phylogenetic status^{10,16}, and/or temperature¹⁷. Since nitrogen fixation is restricted to subtropical gyres, any nutrient thermostat setpoint should be determined by the stoichiometry of phytoplankton living in the subtropical gyres $((N:P)_p)$ ¹⁸. We hypothesize that variations in elemental stoichiometry of N, P, and Fe will fundamentally change the linkages between these three cycles and how they influence net primary productivity, carbon export, and deep ocean nutrient inventories.

Building on the framework outlined by Tyrrell, we constructed a simple box model with only 11 variables, incorporating the cycling of three nutrients, three phytoplankton types, and regional differences in ecosystem structure, to illustrate the importance of both nutrient supply and demand ratios. The model structure is shown in Figure 1, and it includes two surface boxes to capture ecological and physical differences between high and low-latitude regions, and also models the populations of diazotrophs, small, and large phytoplankton. This simple modeling

framework is advantageous as it provides a clear mechanistic understanding of the influence of varying supply and demand of nitrogen, phosphorus, and iron on biogeochemical cycling and primary productivity, without using a complex model with many poorly constrained parameters.

Our analysis illustrates that all three nutrients can be the *ultimate limiting nutrient*. At equilibrium, there are six nutrient limitation scenarios that support the survival of all three phytoplankton types. In each scenario, low-latitude phytoplankton are limited by N, diazotrophs are limited by either P or Fe, and high-latitude phytoplankton are limited by either P, Fe, or N. For given external nutrient fluxes, which are defined by Equation 1, the realized pattern is determined by the nutrient with the lowest supply-to-demand ratio (equations 2 and 5). Equations 7 through 8 show that primary productivity is a linear function of the supply of each of the nutrients to the box in which they limit a phytoplankton population, with the coefficient of proportionality in each case a function of phytoplankton nutrient ratios. Figures 2 (a) and (b) show how nutrient supply and demand control nutrient limitation patterns by examining the effects of iron deposition on primary productivity. When low-latitude iron deposition is low, diazotrophs are iron-limited and deep ocean nitrogen is low. Iron will be an ultimate limiting nutrient in the low-latitude region, and low-latitude iron and high-latitude nitrate are the ultimate limiting nutrients. As low-latitude iron is increased, deep ocean nitrogen increases and there is an N-teleconnection between the low and high-latitude regions, leading a transition from nitrogen to iron-limitation of the high-latitude regions. Further increases in low-latitude iron lead to a transition to phosphorus-limitation in low-latitudes. As high-latitude iron is increased, there is a transition from iron to nitrate or phosphorus-limitation in the high-latitude region. Hence, each nutrient has the potential to be an *ultimate limiting nutrient*,

and in general multiple nutrients simultaneously control global primary productivity.

The presence of nitrogen fixers in the low-latitude box couples the nitrogen cycle with either the iron or phosphorus cycle, leveraging the effect of the supply of those nutrients to low-latitude regions and making the P:Fe supply ratio to low-latitudes important for determining the limitation regime. The explicit dependence of low-latitude primary productivity on atmospheric N deposition ($f_{N,L}$) arises due to differences in diazotroph and non-diazotroph stoichiometry¹⁹, which is shown in Figure 2 (c). These ratios explicitly appear in the nitrate flux coefficient, and they only vanish with equivalent elemental composition of diazotrophs and non-diazotrophs. In this unlikely scenario, low-latitude N is not an ultimate limiting nutrient, as was found by Tyrrell, and either P or Fe is the only low-latitude ultimate limiting nutrient. The transition point between Fe and P limitation occurs when the supply Fe:P is equal to the small phytoplankton Fe:P (equation 2). This condition is exact for equal stoichiometries, but still holds approximately when diazotroph N:P:Fe are allowed to vary, as non-diazotroph nutrient demand dominates that of diazotrophs due to their much higher biomass (which is explicitly demonstrated in the S.I. section S3). Diazotrophs have N:P and Fe:P greater than non-diazotrophs²⁰, so we tested the sensitivity of low-latitude primary productivity to low-latitude nitrogen deposition under various stoichiometric scenarios, finding that such nitrogen deposition could influence primary productivity only when $(\text{Fe:N})_d \gg (\text{Fe:N})_p$ and when, as is commonly observed^{8,21,22} diazotrophs are Fe-limited (see Figure 2 (c)).

The lack of nitrogen fixers in high-latitude regions decouples the nitrogen cycle here, and any of the nutrients can be ultimate limiting nutrients in this region. High-latitude phytoplankton

are commonly nitrogen-limited, and our model suggests that global primary productivity can be highly sensitive to the external nitrogen flux ($f_{N,U}$). Unlike sensitivity to $f_{N,L}$ this effect is robust to changes in stoichiometry, as is seen in Figure 2 (d). Our finding that N can be an ultimate limiting nutrient despite the presence of nitrogen fixation is a significant departure from previous theoretical models, which were unable to capture the role of N due to assumed Redfield stoichiometry and lack of representation of diazotroph biogeography.

The geographic restriction of diazotrophs to low-latitude regions means that deep ocean ocean nutrient inventories are tied to the stoichiometry of phytoplankton in the low-latitude regions. We demonstrated this by calculating the iron-flux controls on the deep ocean N inventory at equilibrium (Figure 3 and equation 9). There was a homeostatic connection between the N and other nutrient cycles, as these cycles depend on whether diazotrophs were P or Fe-limited. In the P-limited state, equilibrium occurs when the N:P of supply matches the biological demand from the non-diazotrophic phytoplankton in low-latitude regions. In this state, the setpoint for the deep ocean N inventory is determined by the P inventory and by $(N:P)_p$ -as is seen in other modelling studies¹⁸. However, the strength of this homeostasis is linked to the relative nutrient supply levels to the high and low-latitude regions and mixing times (SI section S6). When nitrogen fixation is Fe-limited, the N inventory is set so that there is a balance between the N supply from the deep ocean and the Fe supply from atmospheric dust (equation 10). Since observed $(N:P)_{\text{deep}}$ are much below those of low-latitude phytoplankton, we suspect that both iron-limitation and long low-latitude mixing times are at important mechanisms in the contemporary ocean. We used observations of global primary productivity and nutrient stoichiometry to find the most plausible levels of iron de-

position and to determine the nutrient limitation regime in the modern ocean. We found that both (Fe, N) and (Fe, Fe) limitation were plausible, with the latter producing the best fit (shown as the red circle in Figure 2 (a), see SI S8 and figure S9).

What happens to primary productivity when there are large, sudden changes in the nutrient fluxes? The discovery of iron-limitation by Martin²³ and the correlated fluctuations in atmospheric pCO₂ with atmospheric dust deposition suggested that global primary productivity could change dramatically after changes in iron flux. It has been difficult to reconcile this theory with the Redfield-Tyrrell paradigm, which would imply a rapid transition to P limitation following any increase in primary productivity. Anthropogenic inputs of nitrate, phosphate, and iron to the ocean have become significant²⁴, and future climate changes may lead to further alterations of these fluxes. To understand the dynamics of global primary productivity, we used numerical experiments to study the dynamic response of the ocean to increases in iron, nitrogen, and phosphorus fluxes. The model parameters of each experiment are marked by the circles in Figure 2 (a), where the red circle is representative of modern ocean conditions as determined by TPP and (N:P)_{deep}, and the initial condition corresponds to the stable equilibrium state with those parameters. The equilibrium state was perturbed by either doubling the iron or phosphorus fluxes or by increasing nitrogen flux to modern levels. As predicted by our theory, primary productivity strongly responds to sudden increases in the supply of the ultimate limiting nutrients, and more than one nutrient can be the ultimate limiting nutrient. Figures 4 (a) and (d) (which corresponds to the modern ocean) show dramatic increases in primary productivity under iron addition, as was hypothesized by Martin²³ and Falkowski⁷, as well as nitrate, which is at odds with current thinking. These responses

Important Variables and Constants	Description
B_d, B_p, B_u	Biomass of diazotrophs, low-latitude phytoplankton, and high-latitude phytoplankton.
Fe_D, Fe_L, Fe_U	Concentration of iron in the deep ocean, low-latitude region, and high-latitude region.
N_D, N_L, N_U	Concentration of nitrogen in the deep ocean, low-latitude region, and high-latitude region.
P_D, P_L, P_U	Concentration of phosphorus in the deep ocean, low-latitude region, and high-latitude region.
k_L, k_H	Mixing rates between the surface and the deep in low and high-latitudes.
τ_L, τ_H	Turnover rates in the low and high-latitude regions due to mixing with the deep.
d_D, d_L, d_H	Depths of the deep ocean, low-latitude region, and high-latitude region.
$(N:P)_d, (N:P)_p, (N:P)_u$	N:P of diazotrophs, low-latitude and high-latitude phytoplankton.
$(Fe:P)_d, (Fe:P)_p, (Fe:P)_u$	Fe:P of diazotrophs, low-latitude and high-latitude phytoplankton.
r_S	Percentage of primary production remineralizes in the surface.
m	Phytoplankton mortality rate.
D_N	Rate of denitrification.
$f_{Fe,L}, f_{Fe,U}$	Atmospheric iron deposition.
$f_{N,L}, f_{N,U}$	Atmospheric nitrogen deposition.
$f_{P,L}, f_{P,U}$	Atmospheric and riverine phosphorus deposition.

would not be possible in a stoichiometrically homogeneous ocean, as phosphorus would become limiting after a small increase in primary productivity. This constraint does not apply in a variable stoichiometry ocean, and primary production shifts to higher N:P. Thus our work reconciles theories in which iron controls both diazotrophy and high-latitude productivity with our understanding of the nitrogen and phosphorus cycles, in particular iron-based explanations of glacial/interglacial pCO₂ levels. Phosphorus additions can also stimulate primary productivity, as happens in Figures 4 (b), (c), and (e), but these increases happen on very long time-scales. In each experiment, the amplitude of TPP increase is constrained by the supply rate of non-limiting nutrients. In some cases a doubling of limiting nutrient flux leads to a quick transition to limitation by a different nutrient and a small increase in primary productivity.

Our conclusions are robust to variations in the model structure and parameters. Other mechanisms not treated by the main model can be important if they change the nutrient supply-to-demand

We present properties of equilibrium solutions in the special case where $(N:P)_p = (N:P)_{deep}$ and $(N:Fe)_d = (N:Fe)_p$, i.e. equal diazotroph and low-latitude phytoplankton stoichiometry. These results are relatively robust to changes in nutrient ratios, a point which we discuss more extensively in the SI. To organize our presentation of the properties of the model at equilibrium, we define the following physical nutrient flux terms:

$$J_{Fe,L} = \frac{1}{\tau_L} (Fe_D - Fe_L) - J_{SC}(Fe_L) + \frac{f_{Fe,L}}{d_L} \quad J_{P,L} = \frac{1}{\tau_L} (P_D - P_L) + \frac{f_{P,L}}{d_L}, \quad (1)$$

with the obvious generalizations defining $J_{Fe,U}$, $J_{P,U}$, $J_{N,L}$, and $J_{N,U}$.

There are six possible nutrient limitation patterns which support the coexistence of all three phytoplankton types at equilibrium. Low-latitude phytoplankton must be limited by N, diazotrophs by Fe or P, and high-latitude phytoplankton by Fe, P or N. The levels of external nutrient flux determine which pattern arises in a given realization. We solved for colimitation conditions to determine which nutrients were limiting. The nutrient limitation pattern must be consistent with the relative geophysical nutrient supply and biological nutrient. In the low-latitude region, diazotrophs are limited by the nutrient with the lowest supply to demand ratio:

$$ULN = \operatorname{argmin}_{Fe,P} (\phi_{Fe,L}, \phi_{P,L}), \quad (2)$$

where $\phi_{Fe,L}$ and $\phi_{P,L}$ are the iron and phosphorus supply rates normalized to demand ratios, defined as follows:

$$\phi_{Fe,L} = J_{Fe,L}(N:Fe)_p \quad \phi_{P,L} = J_{P,L}(N:P)_p \quad (3)$$

$$\phi_{N,U} = J_{N,U} \frac{1 - r_S}{1 + D_N - r_S} \quad \phi_{Fe,U} = J_{Fe,U}(N:Fe)_u \quad \phi_{P,U} = J_{P,U}(N:P)_p \quad (4)$$

In the high-latitude region, we include nitrogen in the expression, and the limiting nutrient is the one whose supply to demand ratio is lowest:

$$ULN = \operatorname{argmin}_{Fe,P,N} (\phi_{N,U}, \phi_{P,U}, \phi_{Fe,U}) \quad (5)$$

For each nutrient limitation pattern, we can solve for the biomass and primary productivity. The biomass of the phytoplankton types and the primary productivity in the subtropical gyre region is given by the following expressions, in the P and Fe cases respectively:

$$B_d = -\frac{J_{N,L}}{m} + \frac{(-r_S + D_N + 1)J_{P,L}(N:P)_p}{(1 - r_S)m}, \quad B_p = \frac{J_{N,L}}{m} + \frac{(r_S - D_N)J_{P,L}(N:P)_p}{(1 - r_S)m}, \quad TPPP_L = \frac{J_{P,L}(N:P)_p}{(1 - r_S)} \quad (6)$$

$$B_d = -\frac{J_{N,L}}{m} + \frac{(-r_S + D_N + 1)J_{Fe,L}(N:Fe)_p}{(1 - r_S)m}, \quad B_p = \frac{J_{N,L}}{m} + \frac{(r_S - D_N)J_{Fe,L}(N:Fe)_p}{(1 - r_S)m}, \quad TPPP_L = \frac{J_{Fe,L}(N:Fe)_p}{(1 - r_S)} \quad (7)$$

Primary productivity and biomass in the upwelling regions are simply determined by the physical supply rate of whichever nutrient is limiting the eukaryotic phytoplankton. If that nutrient is iron, then:

$$TPPP_U = \frac{J_{Fe,U}(N:Fe)_u}{(1 - r_S)} \quad (8)$$

The inputs of iron and phosphorus determine the size of the deep ocean nitrate inventory and $(N:P)_{deep}$. We are particularly interested in $(N:P)_{deep}$ when the ocean is iron replete, as this expression contrasts strongly with the predictions of a Redfieldian ocean. Neglecting small terms, we find the following expression for $(N:P)_{deep}$ in an iron replete ocean:

$$(N:P)_{deep} = (N:P)_p + \frac{D_N}{1 - r_s} \left(-(N:P)_p - \frac{k_U}{k_L} (N:P)_u \right) \quad (9)$$

The corresponding expression for an iron limited ocean is:

$$\frac{N_D}{\tau_L J_{Fe,L}} = (N:Fe)_p - \frac{D_N}{1 - r_s} \left((N:Fe)_p + \frac{J_{Fe,U}(N:Fe)_u}{J_{Fe,L}} \right) \quad (10)$$

Table 1: Properties of equilibrium solutions.

ratios. We performed an extensive analysis of variants of the main model in the SI, in particular testing the effects of variable remineralization rates²⁵, lateral surface nutrient transport¹⁸, and quadratic mortality rates on nutrient limitation patterns and deep ocean nutrient inventory. In section SI S9, we showed how variation in remineralization rates (which allow for each element to have its own ratio of export to recycling) had the same effect as changes in nutrient stoichiometry, and we derived effective resource demand ratios that accounted for variable remineralization. Our results showed that enhanced P-recycling rates strongly enhance the outcome where Fe or N are *ultimate limiting nutrients*.

Our model treats the nutrient ratios of different phytoplankton types as static features, but in reality these parameters are subject to change by physiological adaptation²⁶ or ecological/evolutionary selection^{14,27}. The values of the elemental ratios exert a dominant impact on the biogeochemical predictions of our model, and understanding the ecological constraints on these ratios is paramount in developing a complete theory of biogeochemical cycles over longer time scales. An interesting possibility that is supported by data is that phytoplankton are frugal²⁸ in their resource utilization, increasing their quotas in response to a plentiful resource and reducing their quotas in response to a scarce resource. Such a mechanism would drive the ocean towards colimitation by all three nutrients by shifting both non-diazotroph and diazotroph resource ratios to enhance utilization of any excess nutrients. Thus, evolutionarily constrained by external nutrient inputs to the ocean could be the ultimate regulator of ocean biogeochemistry.

Methods

We created a three box model of the oceans, with each surface box corresponding to the euphotic zone and seasonal thermocline of the subtropical gyres and high-latitude regions, respectively. The model has 11 variables, including the subtropical gyre and high-latitude concentrations of iron, nitrogen, and phosphorus, the deep ocean concentrations nitrogen and phosphorus, and the population levels of diazotrophs, small phytoplankton, and eukaryotic phytoplankton. Within each surface box is embedded an ecosystem model, with each phytoplankton type obeying the Monod equation with Liebig's law of the minimum and a fixed mortality rate. Diazotrophs and small phytoplankton are restricted to the low-latitude regions, whereas eukaryotic phytoplankton are restricted to the high-latitude box. The phytoplankton types couple the nutrient cycles of nitrogen, phosphorus, and iron together via their nutrient stoichiometries, and each phytoplankton type has a fixed ratio of N:P:Fe that is set by consideration of field surveys and laboratory experiments^{10,16,29}. All phytoplankton require phosphorus and iron, but diazotrophs do not take up nitrogen from the environment and are not limited by nitrogen availability. We represent external fluxes of nitrogen, phosphorus and iron into each surface box. Denitrification is represented by the loss of a fixed percentage of remineralized nitrate, and phosphorus loss is modeled by a first order inorganic burial process acting on the deep ocean phosphorus concentration. We assume a constant deep ocean iron concentration, and model the dynamics of upper ocean iron by assuming a fixed concentration of organic ligands, instantaneous equilibrium between ligands and dissolved iron, and first order scavenging losses of dissolved iron.

We studied the behavior of the model by using analytical calculations of equilibrium concentrations of all the nutrients as well as numerical simulations. We performed numerical simulations using the Sundials CVODE implicit solver³⁰, which allowed us to take long time-steps despite the inherent stiffness of our model equations. In order to test the sensitivity of our model results to changes in the different parameters, we computed the gradients of $(N:P)_{\text{deep}}$ and TPP to each of the model parameters, and also performed Monte Carlo simulations to determine the probability distribution of the value of those objective functions when the parameters were drawn from probability distributions reflecting the rough uncertainty of each parameter. We also studied the effect of adding density dependent predation rates on our model solutions. Complete model details, including the results of the sensitivity analysis, are contained in the supplementary information.

Acknowledgements This work was partially supported by NSF Dimensions of Biodiversity grant OCE-1046001 and OCE-1046297 (S.A.L., A.C.M.), Army Research Office Grant W911NG-11-1-0385 (GIH, SAL). The authors do not have any competing financial interests. Correspondence regarding this article should be directed to Adam C. Martiny (amartiny@uci.edu). The research in this paper was designed by A.C.M. and S.A.L., numerical simulations and theoretical calculations were performed by G.I.H., the paper was written by G.I.H., S.A.L., and A.C.M. We acknowledge Francois Primeau for providing thoughtful discussion as well as suggestions.

References

1. Redfield, A. C. The biological control of chemical factors in the environment. *Am. Sci.* **45**, 205–221 (1958).

2. Tyrrell, T. The relative influences of nitrogen and phosphorus on oceanic primary production. *Nature* **400**, 525–531 (1999).
3. Ryther, J. H. & Dunstan, W. M. Nitrogen, Phosphorus, and Eutrophication in the Coastal Marine Environment. *Science* **171**, 1008–1013 (1971).
4. Smith, S. V. Phosphorus versus nitrogen limitation in the marine environment. *Limnol. and Oceanogr.* **29**, 1149–1160 (1984).
5. Lenton, T. M. & Watson, A. J. Redfield revisited: 1. Regulation of nitrate, phosphate, and oxygen in the ocean. *Glob. Biogeochem. Cycles* **14**, 225–248 (2000).
6. Lenton, T. M. & Klausmeier, C. A. Biotic stoichiometric controls on the deep ocean N:P ratio. *Biogeosciences* **4**, 417–454 (2007).
7. Falkowski, P. G. Evolution of the Nitrogen-Cycle and Its Influence on the Biological Sequestration of CO₂ in the Ocean. *Nature* **387**, 272–275 (1997).
8. Moore, C. M. *et al.* Large-scale distribution of Atlantic nitrogen fixation controlled by iron availability. *Nature Geosci.* **2**, 867–871 (2009).
9. Weber, T. S. & Deutsch, C. Ocean nutrient ratios governed by plankton biogeography. *Nature* **467**, 550–554 (2010).
10. Martiny, A. C. *et al.* Strong latitudinal patterns in the elemental ratios of marine plankton and organic matter. *Nature Geosci.* **6**, 279–283 (2013).

11. Teng, Y., Primeau, F. W., Moore, J. K., Lomas, M. W. & Martiny, A. C. Global-scale variations of the ratios of carbon to phosphorus in exported marine organic matter. *Nature Geosci.* **7**, 895–898 (2014).
12. Schlosser, C. *et al.* Seasonal ITCZ migration dynamically controls the location of the (sub)tropical Atlantic biogeochemical divide. *Proc. Natl. Acad. Sci. U.S.A.* **111**, 1438–42 (2014).
13. Snow, J. T. *et al.* Environmental controls on the biogeography of diazotrophy and Trichodesmium in the Atlantic Ocean. *Glob. Biogeochem. Cycles* **29**, 865–884 (2015).
14. Klausmeier, C. A., Litchman, E., Daufresne, T. & Levin, S. A. Optimal nitrogen-to-phosphorus stoichiometry of phytoplankton. *Nature* **429**, 171–174 (2004).
15. Klausmeier, C. A., Litchman, E., Daufresne, T. & Levin, S. A. Phytoplankton stoichiometry. *Ecol. Res.* **23**, 479–485 (2008).
16. Quigg, A. *et al.* The evolutionary inheritance of elemental stoichiometry in marine phytoplankton. *Nature* **425**, 291–4 (2003).
17. Toseland, A. *et al.* The impact of temperature on marine phytoplankton resource allocation and metabolism. *Nature Clim. Change* **3**, 979–984 (2013).
18. Weber, T. & Deutsch, C. Oceanic nitrogen reservoir regulated by plankton diversity and ocean circulation. *Nature* **489**, 419–22 (2012).
19. Berman-Frank, I., Cullen, J. T., Shaked, Y., Sherrell, R. M. & Falkowski, P. G. Iron availability, cellular iron quotas, and nitrogen fixation in Trichodesmium. *Limnol. Oceanogr.* **46**, 1249–1260 (2001).

20. Kustka, A., Sañudo-Wilhelmy, S., Carpenter, E. J., Capone, D. G. & Raven, J. A. A revised estimate of the iron use efficiency of nitrogen fixation, with special reference to the marine cyanobacterium *Trichodesmium* spp.(Cyanophyta) 1. *J. of Phyco.* **39**, 12–25 (2003).
21. Mills, M. M., Ridame, C., Davey, M., La Roche, J. & Geider, R. J. Iron and phosphorus co-limit nitrogen fixation in the eastern tropical North Atlantic. *Nature* **429**, 292–4 (2004).
22. Boyle, E. A., Bergquist, B. A., Kayser, R. A. & Mahowald, N. Iron, manganese, and lead at Hawaii Ocean Time-series station ALOHA: Temporal variability and an intermediate water hydrothermal plume. *Geochim. Cosmochim. Acta* **69**, 933–952 (2005).
23. Martin, J. H., Gordon, M. & Fitzwater, S. E. The case for iron. *Limnol.and Oceanogr.* **36**, 1793–1802 (1991).
24. Duce, R. A. *et al.* Impacts of atmospheric anthropogenic nitrogen on the open ocean. *Science* **320**, 893–7 (2008).
25. Monteiro, F. M. & Follows, M. J. On nitrogen fixation and preferential remineralization of phosphorus. *Geophysical Research Letters* **39** (2012).
26. Bonachela, J. A., Klausmeier, C. A., Edwards, K. F., Litchman, E. & Levin, S. A. The role of phytoplankton diversity in the emergent oceanic stoichiometry. *J. Plankton Res.* (2015).
27. Karl, D. M. A sea of change: Biogeochemical variability in the North Pacific subtropical gyre. *Ecosystems* **2**, 181–214 (1999).

28. Galbraith, E. D. & Martiny, A. C. A simple nutrient-dependence mechanism for predicting the stoichiometry of marine ecosystems. *Proc. Natl. Acad. Sci. U.S.A.* **112**, 8199–8204 (2015).
29. Ho, T. Y. *et al.* The elemental composition of some marine phytoplankton. *J. of Phycol.* **39**, 1145–1159 (2003).
30. Hindmarsh, A. C., Brown, P. N. & Grant, K. E. SUNDIALS: Suite of nonlinear and differential/algebraic equation solvers. *ACM Transactions on Mathematical Software (TOMS)* **31**, 363–396 (2005).

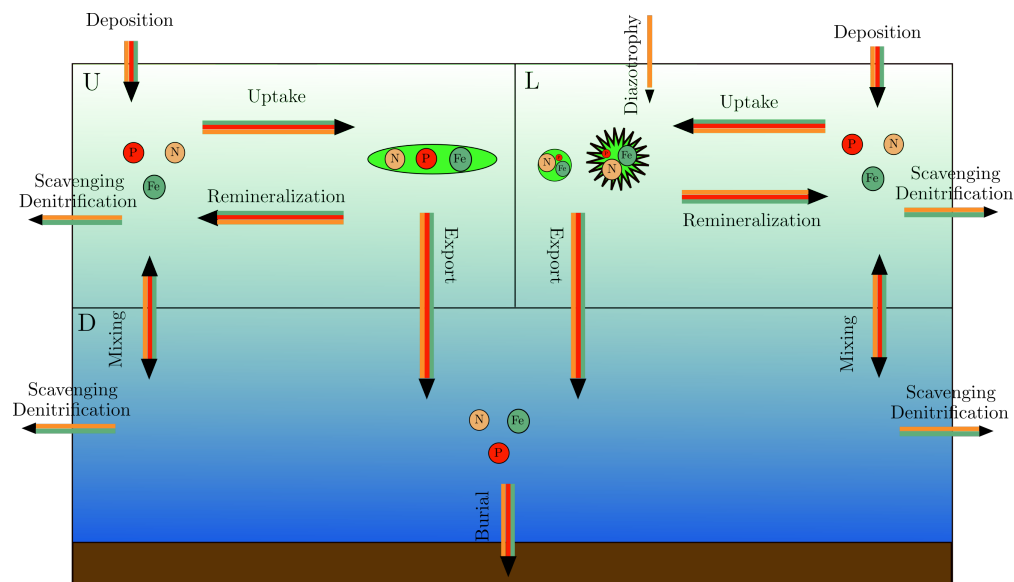


Figure 1: Multi-box model of ocean biogeochemistry. The upper ocean is divided into two boxes, one of which contains diazotrophs and the other which does not. The boxes represent highly stratified, warm water, subtropical gyres and cold water upwelling regions, respectively. The phytoplankton in each box have unique stoichiometric ratios and the boxes have varying levels of upwelling and nutrient deposition.

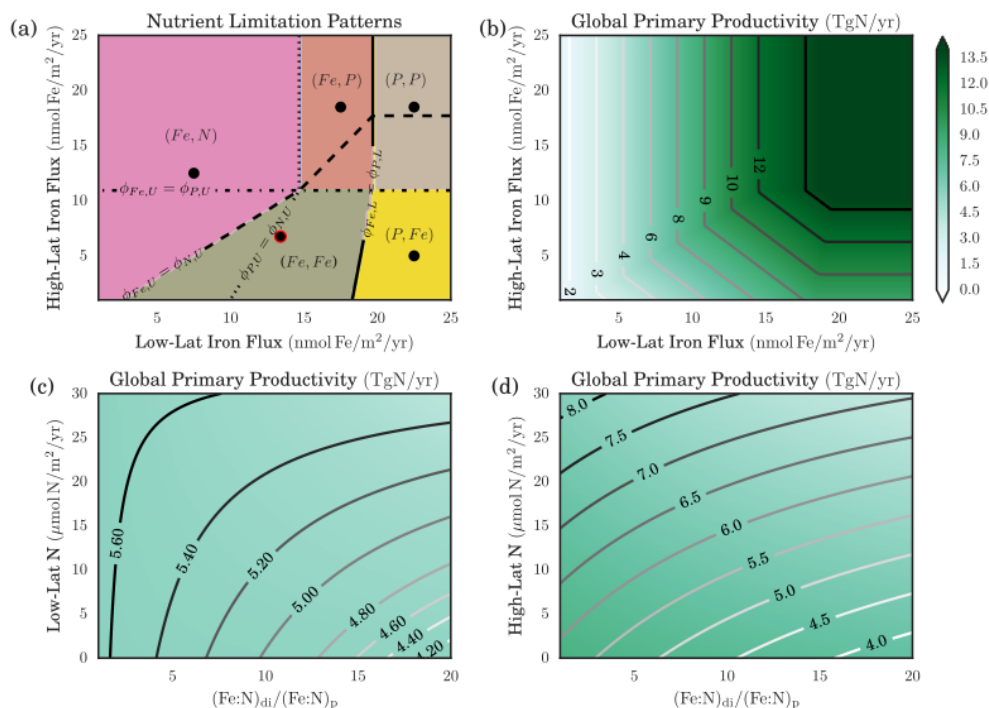


Figure 2: Influence of varying ocean conditions on nutrient limitation (a) and primary productivity (b) through (d). Figure (a) shows the ultimate limiting nutrients as a function of iron deposition rates in both high and low-latitudes. The set of ultimate limiting nutrients are determined by relative nutrient supply and demand. The black contours show the points where relative supply and demand for two different nutrients are equal to each other, implying a potential transition in the ultimate limiting nutrient. Figure (b) shows the impact of iron levels on primary productivity. Figures (c) and (d) show that impact of high and low-latitude nitrate supply and diazotroph iron content on primary productivity. In each case, the simulations were performed when low-latitude iron was an ultimate limiting nutrient.

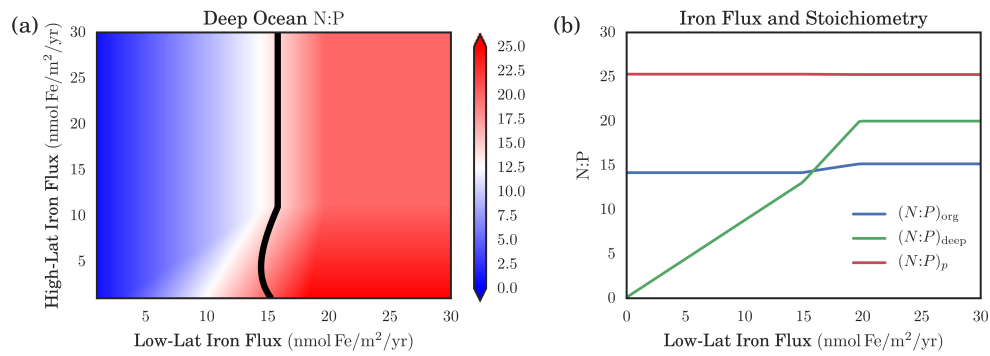


Figure 3: The effect of iron deposition on nutrient ratios in the ocean. Figure (a) shows $(N:P)_{deep}$ as a function of high and low-latitude iron deposition. The black contour is the set of points where $(N:P)_{org} = (N:P)_{deep}$. Figure (b) shows $(N:P)_{deep}$, $(N:P)_{org}$, and low-latitude $(N:P)_{org}$, as iron deposition is increased throughout the ocean.

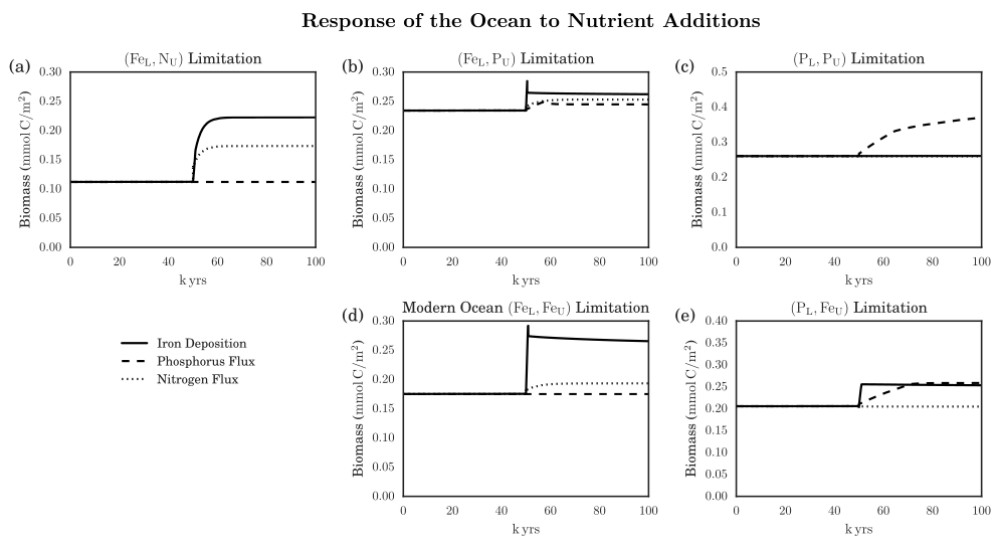


Figure 4: Response of the ocean to increases of the nitrate, phosphate, and iron fluxes in different nutrient limitation regimes. Each figure corresponds to a numerical experiment with parameters selected from the marked locations in Figure 2. Figure (d) corresponds to both the (Fe, Fe) limitation regime and our best estimate of the modern ocean.